SAND2019-14842C

Performance of AeroMINEs for Distributed Wind Energy

Suhas Pol[1]
Texas Tech University, Lubbock, Texas, 79409, USA

Brent C. Houchens[2] and David V. Marian[3]
Sandia National Laboratories, Livermore, California, 94550, USA

Carsten H. Westergaard[4]
Westergaard Solutions Inc., Houston, Texas, 77006, USA

AeroMINE (Motionless, INtegrated Extraction) wind harvesters provide distributed power generation with no external moving parts. Their patent-protected design easily integrates into buildings and can operate stand-alone or in conjunction with rooftop solar photovoltaics. Here, the AeroMINE configuration of a single-pair of opposing foils is investigated in wind tunnel tests. Through various geometric optimizations (foil spacing, angle-of-attack and air-jet configuration) a mechanical efficiency of approximately 1/3 of the Betz limit is achieved. Intermittent operation at significantly higher efficiency (approaching ½ of the Betz limit) is demonstrated for higher angles-of-attack, but steady operation is impeded by an aerodynamic instability. In addition to pressure and anemometry, particle image velocimetry is utilized to characterize the flow around and through the AeroMINE pair.

I. Nomenclature

A_{exit}	=	exit area (largest dimension) of unit
A_{jet}	=	total area of air-jets (orifices) in foil surface
AoA	=	angle-of-attack (half-angle between foils)
CFD	=	computational fluid dynamics
$c_p(x)$	=	representation of surface pressure on foils
Δp_{jet}	=	pressure-drop over jets
Δp_{choke}	=	pressure-drop over jets
γ	=	representative jet discharge coefficient
L	=	chord length
LCOE	=	levelized-cost-of-electricity
$Power$	=	power of the AeroMINE unit
PIV	=	particle image velocimetry
PV	=	photovoltaic
ρ	=	air density
Re	=	Reynolds number based on chord
u_{jet}	=	flow velocity at the air-jets
U_∞	=	free-stream velocity
V_{jet}	=	total volume flow through all air-jets

[1] Research Assistant Professor, Department of Mechanical Engineering.
[2] Principal Mechanical Engineer, Department of Thermal-Fluids Sciences and Engineering, AIAA Senior Member.
[3] Product Design Engineer, Department of Mechanical Design and Additive Manufacturing.
[4] President, AeroMINE Power.

II. Introduction

AeroMINE (Aero Motionless, INtegrated Extraction) distributed wind power generators have no external moving parts and easily integrate into buildings (Fig. 1a). By sweeping a large area of wind with a reliable design, AeroMINEs overcome the challenges that have plagued other distributed wind solutions and have hindered distributed wind from playing a significant role in energy markets [1].

Incident wind creates low-pressure regions between the mirrored airfoil-pairs, and this suction pulls air from orifices (air-jets) in the skins of the foils, from the hollow airfoil interiors, supplied by a manifold which incorporates a turbine-generator (Fig. 1b). The turbine-generator is located inside the building, away from extreme weather conditions and protected from people and animals. The patented (and patent-pending) design of AeroMINEs are modular and scalable [2, 3]. They complement rooftop solar photovoltaics (PV) as shown in Fig. 1a. Additional details on AeroMINE operation, including the performance optimization, are available in Houchens *et al.* [4].

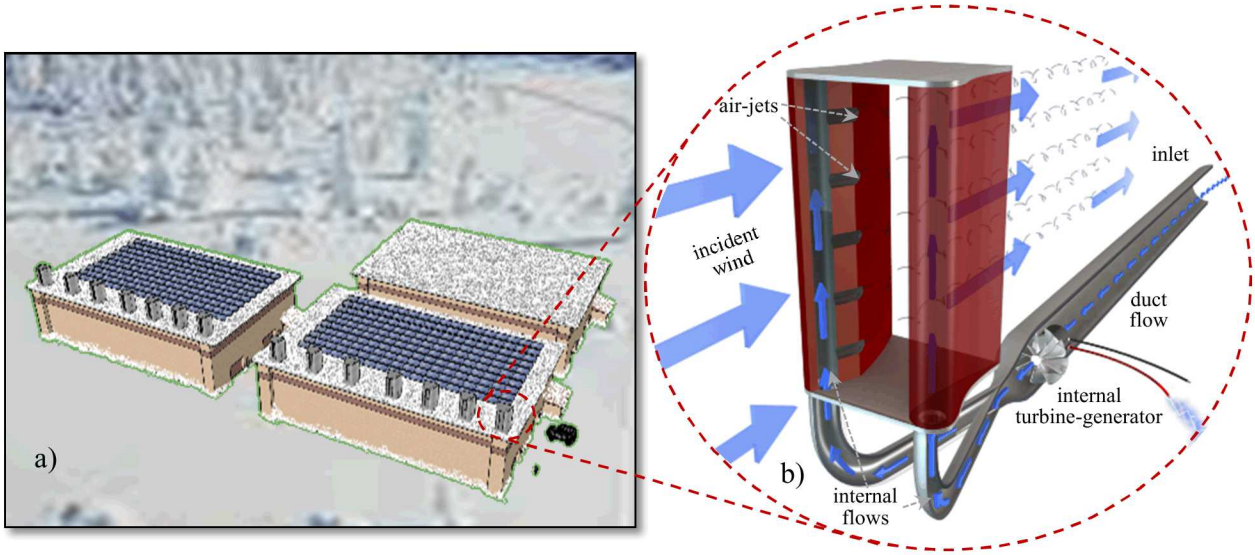

Fig. 1 Renderings of a) 14 AeroMINE pairs on warehouses coupled with a 180 solar PV panels as a functional distributed energy system for inclement settings, and b) schematic of operation of an AeroMINE pair.

III. Experiments

Experiments were conducted in Texas Tech University's National Wind Institute recirculating wind tunnel shown in Fig. 2 (with two 1/6-scale AeroMINEs mounted in parallel from a different study). The cross-section of the tunnel test-section is 1.22 m high x 1.83 m wide (4-feet high by 6-feet wide). The wall on the backside of the tunnel (Fig. 2a) hinges down for mounting the AeroMINEs in a fixture which allows reproducible variations of the angle-of-attack (AoA) of the foils, spacing between a pair of foils, and spacing between multiple devices mounted in parallel. This fixture also allows mounting at off-axis orientations to investigate the impact on efficiency of off-axis incident wind. The opposite side of the test section (Fig. 2b) is transparent, allowing particle image velocimetry (PIV) using a laser mounted downstream of the test section and an external camera array. The tunnel is seeded with oil droplets for this purpose.

Here 1/3-scale (based on chord) single-pair AeroMINE was tested. The foil dimensions were 0.5 m chord and 0.8 m height (mounted sideways as shown in Fig. 3). Small rib sections containing static pressure taps were inserted in the middle of the device as shown in green in Fig. 3. Tubes were run from the taps to outside the wind tunnel for pressure measurements, and a reference static tap was placed at the inner wall of the wind tunnel near the corner. Pressures were measured at five locations along the low-pressure sides of both of the foils. The S1210-based design was selected for its excellent lift characteristics over a wide range of Reynolds numbers [5]. However, as will be shown, the performance changes dramatically due to the presences of the second mirrored foil, even when all of the air-jets are covered.

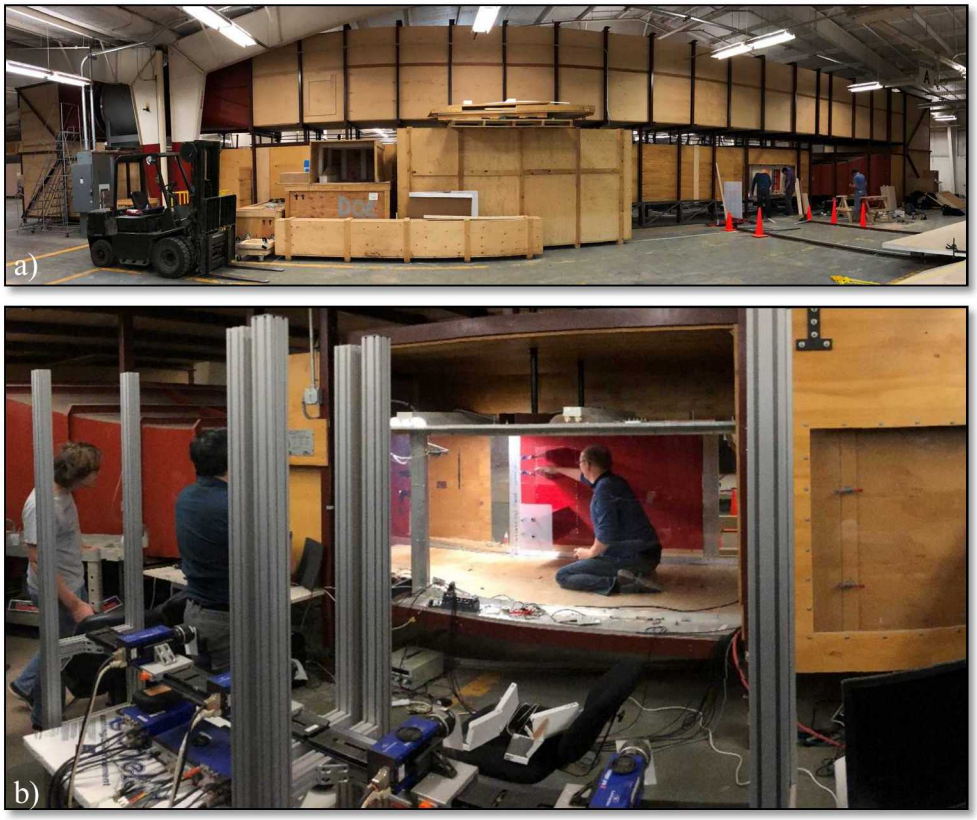

Fig. 2 Wide-angle photos of the National Wind Institute wind tunnel including a) the backside and b) the PIV camera array on the transparent side, looking into a smaller array of two AeroMINE pairs.

Testing on the rapid prototyped foils was performed at freestream velocities between 5 and 15 m/s, corresponding to chord-based Reynolds number (*Re*) between ~130,000 and 400,000, respectively. Results are shown for both 10° or 15° AoA, previously determined to be near optimum performance based on the measured inlet duct velocity [4]. The velocity was measured forward of the AeroMINE and just off the wall of the wind tunnel with a vane anemometer. This was taken as the freestream value U_∞. The proximity of this measurement to the wall is expected to make this representative, or slightly lower (conservative), of the average velocity seen by the AeroMINE pair.

Fig. 3 A 0.5 m chord AeroMINE pair mounted in the wind tunnel. The green ribs contain static pressure taps along the low-pressure side of the foils.

The foil pressure profiles were sampled along the low-pressure sides of the foils via static pressure taps in the green insert shown in Fig. 3. A choke was placed at the inlet flow to the duct to simulate the load of the turbine-generator (Fig. 4). The constriction of the choke was varied to produce a power curve.

Pressures were measured on either side of a choke near the duct inlet and the average velocity was measured inside the duct, allowing calculation of a mechanical power, as shown in Fig. 4. The choke simulates the turbine-generator under various loading conditions. Additionally, PIV measurements of the flow field were taken to better understand the acceleration between the foils and the wake structure.

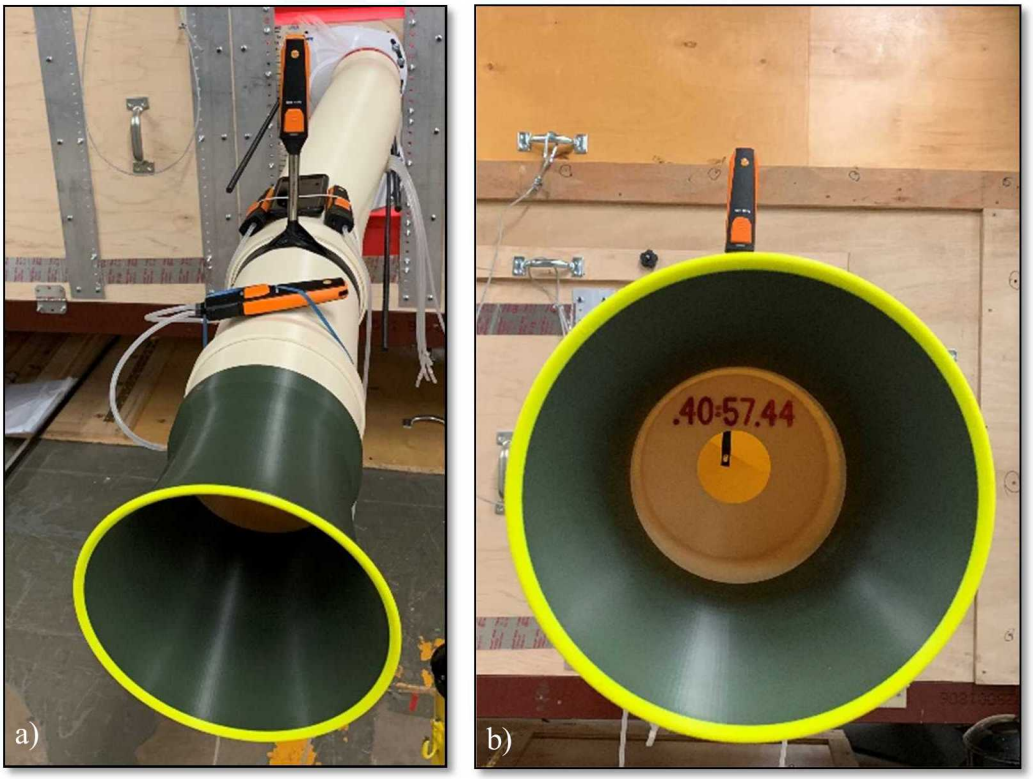

Fig. 4 a) Duct inlet outside the wind tunnel with choke section and b) close-up view down the inlet of the choke and hot wire anemometer.

Blockage measurements showed acceptable impact of the device on the freestream velocity in the adjacent portion of the tunnel. The speed in the tunnel adjacent to the device was measured to be between 10% and 13.5% higher than the freestream values. This was true for both the full-length (0.8 m) and a half-length (0.4 m) devices suggesting that the primary increase in this velocity over the assumed freestream U_∞ is actually due to the freestream measurement location being closer to the wall. This is consistent with measuring a conservative estimate for the freestream U_∞, which is used to determine the efficiency.

IV. Results and Discussion

First the pressure profiles of just the foils with all air-jets closed are presented. In this configuration the AeroMINE produces no power and there is no flow in the inlet. Strong asymmetries thought to result from a flow instability are observed in this no-power configuration.

Then the air-jets are opened allowing the system to produce power. The reduction of asymmetries with a choke load are presented. Then mechanical efficiency of the system is discussed. Together these provide an estimate of potential full-scale system efficiency and insights into sensitivity to flow instabilities which limit the maximum viable AoA for steady performance.

A. All Air-jets Closed – No-Power Configuration

With all air-jets closed (taped over) the pressure at five locations on the low-pressure side of both foils was measured. For convenience of explanation the foils are referenced here as "top" and "bottom" based on there relative position on the wall. The pressure values for two realizations are shown in Fig. 5. Both realizations showed strong asymmetry, with one foil maintaining a much higher pressure far from the leading edge. Initially there was concern that the system was not aligned properly in the tunnel. However, after multiple realizations it was observed that the asymmetry switched side (second realization shown), suggesting this is the result of a flow instability.

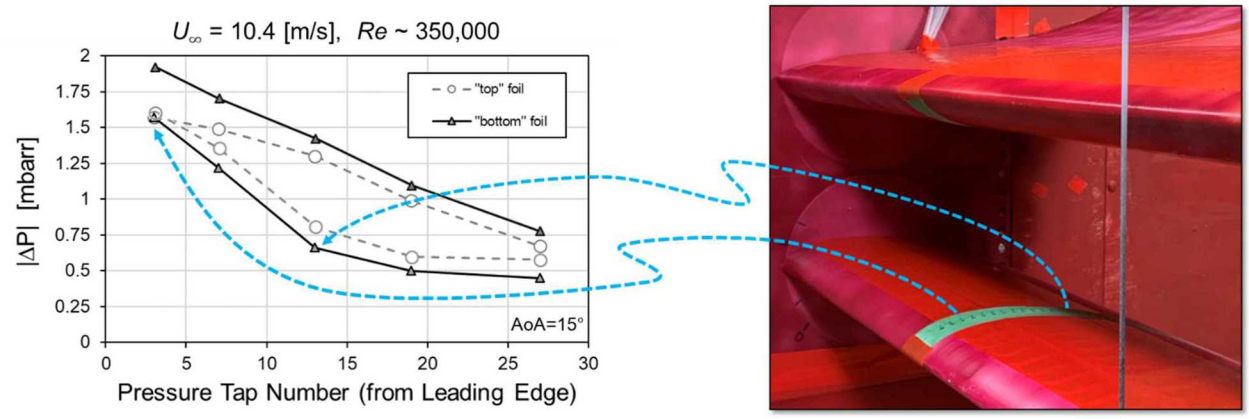

Fig. 5 Pressure tap measurements for two realizations for the "top" and "bottom" foils with all air-jets closed (no-power) at AoA = 15° and U_∞ = 10.4 m/s. Note that the taps do not extend to the trailing edge.

This asymmetry was observed even for AoA = 10° with all air-jets closed as shown by PIV data in in Fig. 6. Note the zero-velocity portion below the "lower" airfoil in the PIV data is due to the support which can be seen in Fig. 3. Some artifacts from the mounts are also visible near the foils.

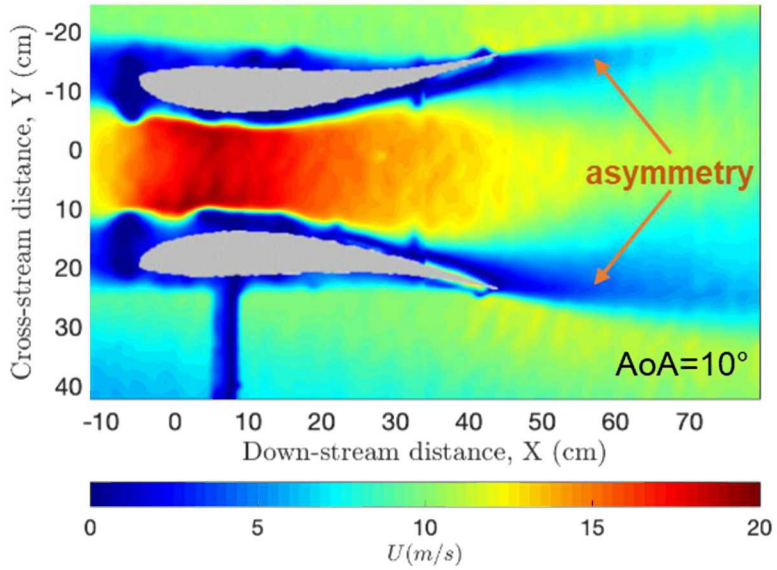

Fig. 6 PIV sampling in a plane aligned with the chord with all air-jets closed (no-power) at AoA = 10° and U_∞ = 10.4 m/s.

B. Air-jets Open – Pressures, PIV and Mechanical Efficiency

With the air-jets open, various chokes were explored. When the choke is fully open (no-choke), air is pulled from outside the wind tunnel through the inlet (shown in Fig. 4), moves through the foil internal ducts, exits through the air-jets and mixes into the freestream flow. Though the air-jets are operational, without a choke there is no load on

system. The pressures along the foils are shown in Fig. 7 for AoA = 15° and AoA = 10°. In general the asymmetry is reduced with the air-jets operational as compared to the all air-jets closed scenario. Some asymmetry still occurs in the AoA = 15° case, with the realization shown here considered a typical case. The asymmetry is reduced by reducing the AoA to 10°, but this comes at a price of sweeping less area of the incident wind and thus reducing the potential power available.

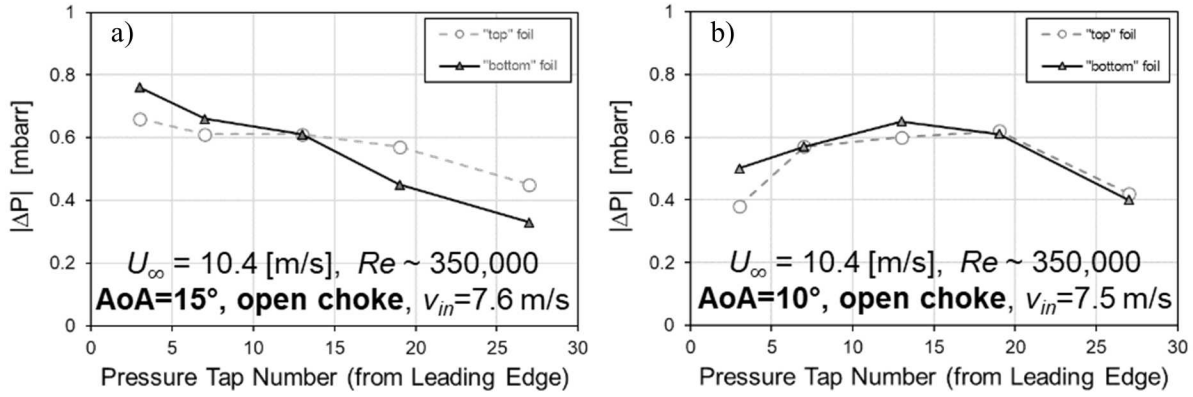

Fig. 7 Pressure tap measurements for the "top" and "bottom" foils with air-jets operational and no-choke (open inlet), for U_∞ = 10.4 m/s and a) AoA = 15° and b) AoA = 10°.

When a choke, representative of the internal turbine-generator, is included, symmetry is greatly improved. This can be seen from the PIV data in Fig. 8 for AoA = 10° where the no-choke and choked flows are shown. As the choked scenario represents the most realistic operational design, this improvement in symmetry is highly beneficial to the practical design.

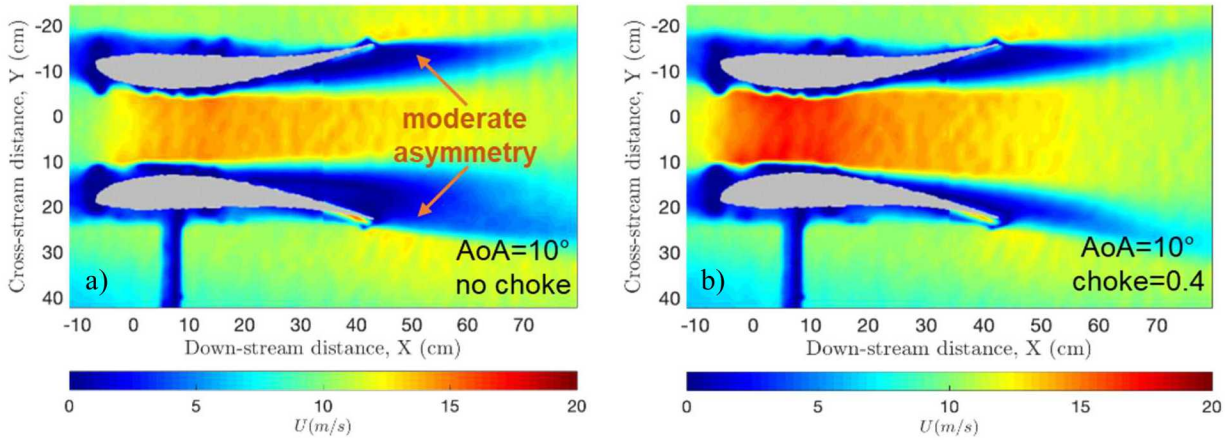

Fig. 8 PIV data for U_∞ = 10.4 m/s and AoA = 10° showing the a) no-choke scenario and b) improved symmetry when a load is applied via a choke at the inlet of the AeroMINE.

Finally, the mechanical efficiency provides a measure of the maximum power extraction. By varying the size of the choke it is possible to produce a power curve for the system. The mechanical power was calculated using the measured pressure drop across the choke, multiplied by the duct area and the average duct velocity

$$Power = \Delta P_{choke} \times A_{duct} \times u_{duct} .$$

The power available for extraction from the wind in the swept area of the AeroMINE in the wind tunnel represents the maximum possible power of the system. Dividing the *Power* by the maximum possible power gives the efficiency of the system. The peak measured efficiency at AoA = 10° was determined to be 18%, which equates to roughly 1/3 of the Betz limit. The full power curve, measured by changing chokes is shown in Fig. 9.

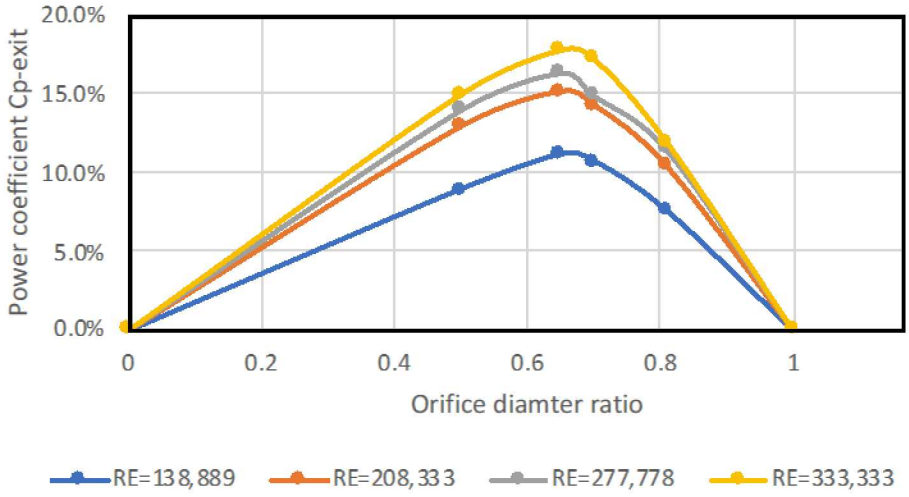

Fig. 9 Power curve for 1/3-scale AeroMINE at AoA = 10° for a range of freestream velocities.

C. Flow Instabilities

Operation at higher AoA than reported in the above section has the potential to increase the energy extraction of the system by producing a lower pressure between the foils. For an individual S1210 foil alone and for *Re* at and above 200,000 the lift continues to increase dramatically up to and past AoA of 20° [5]. Thus, operating at a higher AoA is expected to increase the power of the AeroMINE system.

Note that, in some cases, this increased energy extraction may not offset the increase in swept area, such that while the power produced might increase, the efficiency could decrease due to a more than proportionally larger increase in swept area. Nevertheless, in building installations, the optimum design may correspond to a non-optimum efficiency, driven by capital expenditure and geometric constraints. Thus, higher AoAs were investigated to better understand subtleties of this optimization.

At higher AoA it is observed that AeroMINEs experiences a flow instability not observed for a single S1210 airfoil. Efficiencies at these higher AoAs can reach as high as 27%, but are subject to instabilities which significantly reduce the power production and result in efficiencies around 10%, well below the stable value of 18% observed at lower AoA as shown above. The operating mode associated with the lower efficiency appears to be associated with a stable mode, as recovery to the higher efficiency has not been observed. This instability also appears to be unique to the symmetry-breaking instability observed when all air-jets are closed.

V. Conclusions

At the optimum stable geometric configuration, AeroMINE has achieved an 18% mechanical efficiency based on wind tunnel experiments conducted at the National Wind Institute at Texas Tech University. Asymmetries apparently due to instabilities are present for both scenarios with no air-jets (two mirrored foils alone) and for with air-jets operational but no load applied. Applying a load from a choke improves the symmetry of the flow.

A poorly understood second instability exists at higher AoA. In this configuration up to 27% efficiency can be achieved, but the stable mode is associated with a very low efficiency. Understanding and controlling this instability is the focus of future research efforts.

Acknowledgments

This work was funded in part by awards from the *2017 Sandia Pitch Competition* and subsequent DOE-wide *National Lab Accelerator Pitch Event* to aid in commercialization of promising technologies, as well as a grant from the *GLEAMM Spark Fund* to accelerate the commercialization of energy technologies through gap funding. Laboratory Directed Research and Development (LDRD) funds have also been provided by Sandia National Laboratories through the *2018 Innovation Challenge* initiative of the Environment and Homeland Security Investment Area.

Sandia National Laboratories is a multimission laboratory managed and operated by National Technology & Engineering Solutions of Sandia, LLC, a wholly owned subsidiary of Honeywell International Inc., for the U.S. Department of Energy's National Nuclear Security Administration under contract DE-NA0003525. The views expressed in the article do not necessarily represent the views of the U.S. Department of Energy or the United States Government.

References

[1] Orrell, A. C., Foster, N. F., Morris, S. L. and Homer, J. S. "2016 Distributed Wind Market Report," Prepared for the U.S. Department of Energy Office of Energy Efficiency and Renewable Energy by the Pacific Northwest National Laboratory, 2017.
[2] Westergaard, C.H., Fluid flow energy extraction system and method related thereto, US2017298900, US Patent Office.
[3] Houchens, B.C., Blaylock, M.L., Marian, D.V. Maniaci, D.C. and Westergaard, C.H., Methods, systems, and devices to optimize a fluid harvester, priority app US 16/182,488, 2018.
[4] Houchens, B. C., Marian, D. V., Pol, S. and Westergaard, C. H. "A Novel Energy Conversion Device for Wind and Hydrokinetic Applications," *Proceedings of the ASME-JSME-KSME 2019 Joint Fluids Engineering Conference*, AJKFLUIDS2019- 5542, ASME, San Francisco, CA, 2019.
[5] Selig, M.S., Guglielmo, J.J., Broeren, A.P. and Giguere, P. "Summary of Low-Speed Airfoil Data," Vol. 1, 1995.